

· 专题研究:妇产科疾病 ·

HSG 影像特征联合临床特征诊断宫腔粘连的效能研究

刘 婷¹, 杜子伟¹, 徐文健^{1*}, 鲁景元¹, 李秀玲²

¹南京医科大学附属妇产医院(南京市妇幼保健院)放射介入科, ²生殖医学中心, 江苏 南京 210004

[摘要] 目的: 探讨子宫输卵管造影(hysterosalpingography, HSG)影像特征联合临床因素对宫腔粘连(intrauterine adhesions, IUA)的诊断价值, 并评估其在不同分型中的鉴别效能。方法: 回顾性分析2019年1月—2024年10月在南京医科大学附属妇产医院放射介入科接受HSG检查疑似IUA且完成宫腔镜检查患者的资料。其中HSG疑似IUA患者282例(含164例术前三维超声数据)。应用单因素分析HSG影像特征(如充盈缺损数量及位置、输卵管阻塞、宫腔形态等)及临床特征(宫腔操作史、流产次数、月经量减少等), 将具有统计学意义($P < 0.05$)的变量纳入多因素有序Logistic回归分析, 筛选独立预测因子, 绘制受试者工作特征(receiver operating characteristic, ROC)曲线, 分析HSG影像特征联合临床因素对IUA诊断及分型的价值, 并与三维超声进行对比。结果: 宫腔镜确诊IUA 251例(89.0%), 并基于美国生育协会(American Fertility Society, AFS)分型标准分为无IUA($n=31$), 轻度IUA($n=64$), 中度IUA($n=129$), 重度IUA($n=58$)。分别筛选出临床特征包括人流等, 以及影像学特征包括宫腔充盈缺损等预测因子。诊断IUA的ROC曲线下面积(area under the curve, AUC)为0.920, 灵敏度为87.3%, 特异度为80.7%; 诊断轻度及重度IUA的AUC分别为0.704和0.786, 灵敏度分别为46.9%和77.6%, 特异度分别为87.6%和65.2%。三维超声诊断IUA的灵敏度和特异度分别为81.4%和68.4%。结论: HSG影像特征联合临床因素等多参数指标在宫腔粘连的诊断中具有较高的敏感性和特异性, 尤其在鉴别轻度和重度IUA方面具有较好的效能, HSG可作为无创筛查工具, 为临床分层管理提供了重要依据。

[关键词] 子宫输卵管造影术; 宫腔粘连综合征; 宫腔镜检查; 三维超声; 多因素回归分析

[中图分类号] R711.4

[文献标志码] A

[文章编号] 1007-4368(2026)05-629-08

doi: 10.7655/NYDXBNSN250754

Diagnostic efficiency of HSG imaging features and clinical characteristics in diagnosing intrauterine adhesions

LIU Ting¹, DU Ziwei¹, XU Wenjian^{1*}, LU Jingyuan¹, LI Xiuling²

¹Department of Interventional Radiology, ²Reproductive Medicine Center, Women's Hospital of Nanjing Medical University, Nanjing Women and Children's Healthcare Hospital, Nanjing 210004, China

[Abstract] **Objective:** To explore the diagnostic value of the imaging features of hysterosalpingography (HSG) combined with clinical factors for intrauterine adhesions (IUA), and to evaluate its diagnostic performance in different types of IUA. **Methods:** A retrospective analysis was conducted on the clinical data of patients with suspected IUA who underwent diagnostic HSG at the Department of Intervention Radiology, Women's Hospital of Nanjing Medical University, between January 2019 and October 2024, and subsequently completed hysteroscopy. This cohort included 282 patients suspected of IUA (including 164 with preoperative three-dimensional ultrasound data). Univariate analysis was conducted to evaluate HSG imaging features, including the number and location of filling defects, tubal occlusion, and uterine cavity morphology, as well as clinical characteristics such as history of intrauterine procedures, abortion count, and menstrual flow reduction, etc. Variables demonstrating statistical significance ($P < 0.05$) were subsequently included in multivariate ordinal logistic regression analysis to identify independent predictors. Receiver operating characteristic (ROC) curve analysis was performed to evaluate the diagnostic and classification value of combined HSG imaging features and clinical factors for IUA. This value was further compared with that of three-dimensional ultrasound. **Results:** Hysteroscopy confirmed IUA in 251 cases (89.0%), who were further categorized according to the American Fertility Society (AFS) classification

[基金项目] 江苏省妇幼保健协会科研立项(FYX202010); 南京市卫生科技发展专项基金(YKK22152)

*通信作者(Corresponding author), E-mail: mexuwenjian@163.com (ORCID: 0009-0003-1814-3747)

system into no IUA ($n=31$), mild IUA ($n=64$), moderate IUA ($n=129$), and severe IUA ($n=58$). The predictive factors of clinical features including induced abortion and imaging features including uterine filling defect were screened. For the diagnosis of IUA, the area under the receiver operating characteristic curve (AUC) was 0.920, with a sensitivity of 87.3% and a specificity of 80.7%. The AUC values for diagnosing mild IUA and severe IUA were 0.704 and 0.786, respectively, with sensitivities of 46.9% and 77.6%, and specificities of 87.6% and 65.2%. In comparison, three-dimensional ultrasound has shown a sensitivity of 81.4% and a specificity of 68.4% for diagnosing IUA. **Conclusion:** The combination of HSG imaging features and clinical features through multi-parameter indicators can effectively diagnose IUA and demonstrate good discriminatory efficacy for distinguishing between mild and severe IUA, and serves as a reliable tool for non-invasive screening while providing a basis for clinical stratified management.

[Key words] hysterosalpingography; intrauterine adhesions; hysteroscopy; three-dimensional ultrasound; multivariate logistic regression

[J Nanjing Med Univ, 2026, 46(05): 629-636]

子宫输卵管造影(hysterosalpingography, HSG)作为无创性操作,是检查女性不孕症的经典影像学技术,不仅能客观评估双侧输卵管通畅性,同时还可以观察宫腔形态,在不孕症诊疗中具有独特且重要的价值^[1]。宫腔粘连(intrauterine adhesions, IUA)是子宫内膜基底层损伤后修复异常导致的妇科常见疾病,表现为月经异常及生育力损害,严重影响女性生育健康^[2]。其病因多与相关宫腔操作(如人工流产、上环取环、剖宫产等)有关。Hooker等^[3]的Meta分析显示,接受刮宫术的患者中IUA发生率高达19.1%。目前,宫腔镜检查被视为IUA诊断的“金标准”,兼具诊断和治疗功能^[4]。但由于其为有创性操作,可能导致子宫穿孔、水中毒等并发症,存在一定局限性^[5]。而且通过宫腔镜粘连分离术(transcervical resection of adhesions, TCRA)治疗,中、重度IUA患者的术后复发率仍可达62.5%^[6]。经阴道超声及宫腔三维超声虽经济便捷,但其局限性较多,如高度依赖B超医生的经验、对轻度IUA敏感性较低、宫腔深部显示不清、宫内节育器影响等^[7]。因此亟须发展无创可重复的影像学检查方法,而HSG在评估输卵管通畅性的同时可以对宫腔形态进行评价,目前已经有诸多研究证实HSG对子宫形态发育异常、宫腔占位性病变及IUA的检出具有价值^[8]。尽管单一的HSG检查具有局限性,然而将HSG影像特征与患者的临床因素相结合以诊断IUA,目前尚未有相关报道。因此本研究旨在通过多因素回归分析,整合HSG影像特征及临床高危因素,筛选独立预测因子,并基于美国生育协会(American Fertility Society, AFS)的分型标准,评估预测因子对粘连严重程度的判别效能,为临床提供更经济、高效的诊断策略。

1 对象和方法

1.1 对象

回顾性分析2019年1月—2024年10月于南京市妇幼保健院放射介入科接受HSG检查且提示疑似IUA的患者资料,共计282例。纳入标准如下:①疑似IUA患者均于HSG检查后3个月内接受宫腔镜检查;②HSG影像清晰可辨,包含宫腔形态、输卵管显影及宫腔充盈缺损特征;③临床资料完整记录,包含月经史、生育史及宫腔操作史;④18~45岁育龄期女性。排除标准包括:①合并其他宫腔占位性病变:黏膜下肌瘤、子宫内膜息肉或宫腔异物残留;②生殖系统炎症:急性盆腔炎、子宫内膜炎或术后感染;③影像质量差:HSG影像模糊、宫腔充盈差或宫腔发育异常伪影显著;④严重全身性疾病:如凝血功能障碍、恶性肿瘤或严重心肺疾病;⑤精神疾病或认知障碍患者。本研究已获得南京医科大学附属妇产医院医学伦理委员会审查和批准(批件号:PJ-2025KY047-001)。

1.2 方法

1.2.1 HSG检查

月经干净后3~7 d进行,术前排除妊娠、急性感染及碘过敏史,签署知情同意后进行HSG操作的术前准备^[9]。患者取膀胱截石位,窥器暴露宫颈并常规消毒后,经宫颈口置入一次性子宫造影通水管,球囊导管注气1.5 mL固定,经导管缓慢推注对比剂(罂粟乙碘油注射液10 mL,浓度为0.48 g/mL),在数字化X线透视动态观察(北京岛津有限公司岛津FLEXAVISION数字胃肠机)宫腔充盈形态、充盈缺损特征及输卵管情况,24 h延迟盆腔平片评估对比剂弥散情况^[10],HSG图像由2位经验丰富的影像科医师在盲态(即不知晓患者信息及病史)条件下独

立判读,如遇争议,则由第3位具有15年HSG诊断经验的医生讨论决定。

1.2.2 宫腔镜检查

本研究设计中,HSG检查疑似阳性且接受宫腔镜检查的患者($n=282$)。宫腔镜检查是目前诊断IUA的金标准,可直视下观察宫腔形态、明确粘连性质并进行分型,并且可同时进行手术。宫腔镜检查于HSG后3个月内完成,月经干净后3~7 d,患者取截石位采用静脉麻醉,使用扩宫棒按顺序扩张宫颈,置入硬性宫腔镜。以生理盐水充盈宫腔,进行全面探查,详细记录宫腔内的粘连情况,包括是否存在粘连、粘连的具体位置、程度、范围以及输卵管

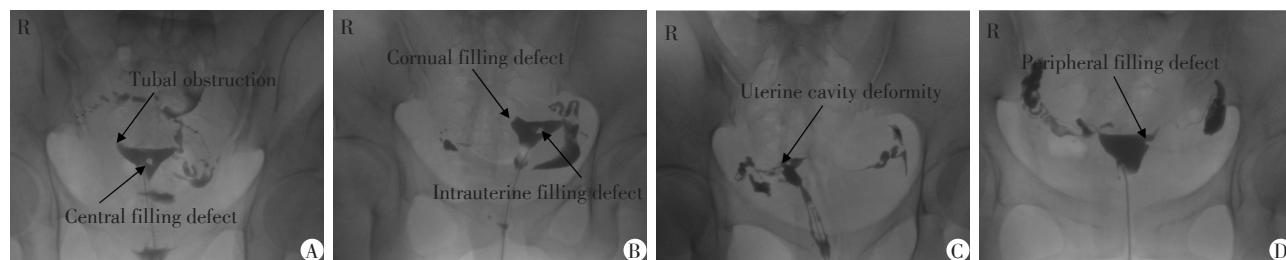
开口的状态等镜下观察结果,在直视下仔细分离粘连,直到恢复正常宫腔形态^[11],根据AFS制定的IUA标准进行诊断分级^[12]。

1.2.3 观察指标

临床因素:年龄、体重指数(body mass index, BMI)、流产次数、剖宫产史、宫腔操作史(如宫腔镜息肉摘除、子宫相关手术史)、孕产史等。HSG影像征象:包括宫腔内对比剂充盈缺损范围、两侧宫角情况、输卵管情况、宫腔形态、两侧宫壁情况等(图1)。

1.3 统计学方法

本研究采用SPSS 27.0软件进行统计分析。连



A: Central filling defect and tubal obstruction. B: Cornual filling defect and intrauterine filling defect. C: Uterine cavity deformity. D: Peripheral filling defect.

图1 HSG影像学特征

Figure 1 HSG imaging features

续变量的正态性通过Shapiro-Wilk检验评估:符合正态分布者以均值±标准差($\bar{x} \pm s$)表示,多组间比较采用单因素方差分析(one-way analysis of variance, one-way ANOVA),进一步两两比较采用Tamhane's T2检验。对于非正态分布的数据,采用中位数(四分位数) $[M(P_{25}, P_{75})]$ 进行描述,组间差异则通过Kruskal-Wallis H 检验进行分析,进一步两两对比使用Mann-Whitney U 检验方法。分类变量以频数(百分率) $[n(\%)]$ 表示,组间比较采用卡方(χ^2)检验,若理论频数 <5 则使用Fisher精确概率法。将具有统计学意义($P < 0.05$)的变量纳入多因素有序Logistic回归分析,预测因子效应以比值比(odds ratio, OR)及95%置信区间(confidence interval, CI)表示。通过多因素回归分析,绘制受试者工作特征(receiver operating characteristic, ROC)曲线以评估不同程度IUA的诊断效能,并计算曲线下面积(area under the curve, AUC)及其95% CI。

2 结果

2.1 临床特征

本研究共纳入282例HSG检查疑似IUA患者,

经宫腔镜检查确诊IUA 251例(89.0%)。根据AFS IUA分型标准将IUA分为轻度($n=64$)、中度($n=129$)、重度($n=58$)和无粘连($n=31$)4组。4组患者的年龄、BMI及孕产史差异均无统计学意义,流产次数及临床症状差异均有统计学意义(表1)。

2.2 影像特征单因素分析及多因素Logistic分析

单因素分析影像特征显示,宫腔轮廓不规则、充盈缺损的数量及位置,以及输卵管阻塞情况鉴别不同程度IUA影像学特征均表现出统计学上的显著差异(表2)。对具有统计学意义的临床及影像特征变量纳入多因素有序Logistic回归分析,发现6项与IUA分型显著相关的独立预测因子($P < 0.05$),其中中央型充盈缺损($OR=12.147, 95\%CI: 3.544\sim 41.677$)及边缘型充盈缺损($OR=6.606, 95\%CI: 2.029\sim 21.462$)的关联性最强(表3)。

2.3 HSG影像特征联合临床特征对IUA的诊断价值

根据6项预测因子,绘制诊断IUA的ROC曲线及计算AUC。结果显示,诊断IUA的AUC为0.920,灵敏度为87.3%,特异度为80.7%;诊断重度IUA的AUC值为0.786,灵敏度及特异度分别为77.6%、65.2%(表4,图2)。

表1 临床特征单因素分析

Table 1 Univariable analysis of clinical characteristics

Indicator	No adhesion (n=31)	Mild adhesion (n=64)	Moderate adhesion (n=129)	Severe adhesion (n=58)	F/ χ^2	P
Age(years, $\bar{x} \pm s$)	32.5 \pm 0.7	32.4 \pm 0.5	33.0 \pm 0.4	32.0 \pm 0.6	0.722	0.539
BMI[kg/m ² , M(P ₂₅ , P ₇₅)]	22.7(20.4, 24.6)	22.2(20.3, 25.0)	23.0(20.7, 24.9)	22.1(20.5, 24.8)	2.061	0.560
Prior abortion[n(%)]						
\geq 1 time	22(71.0)	45(70.3)	108(83.7)	53(91.4)	11.386	0.010
\geq 2 times	12(38.7)	24(37.5)	63(48.8)	30(51.7)	3.704	0.295
\geq 3 times	5(16.1)	11(17.2)	25(19.4)	12(20.7)	0.418	0.936
Uterine procedure[n(%)]						
Polypectomy	6(19.4)	14(21.9)	16(12.4)	9(15.5)	3.161	0.367
Other uterine surgery	3(9.7)	6(9.5)	7(5.4)	3(5.2)	1.778	0.620
Obstetric history[n(%)]						
Nulliparity	20(64.5)	42(65.6)	70(54.3)	33(56.9)	2.816	0.421
Vaginal delivery	7(22.6)	12(18.8)	38(29.5)	18(31.0)	3.400	0.334
Cesarean section	4(12.9)	10(15.6)	21(16.3)	7(12.1)	0.684	0.877
Clinical symptom[n(%)]						
Hypomenorrhea	9(29.0)	21(32.8)	71(55.0)	35(60.3)	16.473	<0.001
Infertility	5(16.1)	35(54.7)	46(35.7)	16(27.6)	16.764	<0.001
Pelvic pain	2(6.5)	4(6.3)	7(5.4)	4(6.9)	3.726	0.293

表2 影像特征单因素分析

Table 2 Univariable analysis of imaging characteristics

Indicator	No adhesion (n=31)	Mild adhesion (n=64)	Moderate adhesion (n=129)	Severe adhesion (n=58)	F/ χ^2	P
Irregular uterine contour[n(%)]	8(25.8)	37(57.8)	76(58.9)	25(43.1)	13.687	0.003
Irregular contrast pooling[n(%)]	10(32.3)	25(39.1)	66(51.2)	22(37.9)	5.915	0.116
Abnormal uterine shape[n(%)]	4(12.9)	6(9.4)	21(16.3)	13(22.4)	4.145	0.246
Number of filling defects[n(%)]						
Single	11(35.5)	40(62.5)	64(49.6)	24(41.4)	8.290	0.040
Multiple	1(3.2)	13(20.3)	58(45.0)	34(58.6)	37.671	<0.001
Location of defects[n(%)]						
Peripheral	6(19.4)	36(56.3)	79(61.2)	24(41.4)	20.678	<0.001
Central	4(12.9)	17(26.6)	43(33.3)	34(58.6)	23.107	<0.001
Tubal occlusion[n(%)]						
None	26(83.9)	38(59.4)	85(65.9)	28(48.3)	11.973	0.007
Unilateral	4(12.9)	24(37.5)	40(31.0)	19(32.8)	6.108	0.106
Bilateral	1(3.2)	2(3.1)	4(3.1)	11(19.0)	19.346	<0.001

表3 多因素有序Logistic分析

Table 3 Multivariable ordinal logistic regression analysis

Indicator	B	SE	Wald χ^2	P	OR	95%CI
Hypomenorrhea	1.330	0.359	13.767	<0.001	3.782	1.874-7.637
Infertility	1.133	0.368	9.472	0.002	3.105	1.508-6.383
Multiple filling defects	1.337	0.635	4.429	0.035	3.807	1.096-13.236
Bilateral tubal occlusion	1.635	0.546	8.971	0.003	5.128	1.759-14.974
Peripheral filling defect	1.887	0.602	9.840	0.002	6.606	2.029-21.462
Central filling defect	2.497	0.629	15.784	<0.001	12.147	3.544-41.677

表4 HSG影像特征联合临床特征对宫腔粘连的诊断价值

Table 4 Diagnostic efficacy of integrated HSG imaging features and clinical characteristics for IUA

Indicator	AUC	95%CI	P	Sensitivity(%)	Specificity(%)
No adhesion(n=31)	0.920	0.868-0.973	<0.001	87.3	80.7
Mild adhesion(n=64)	0.704	0.629-0.779	<0.001	46.9	87.6
Moderate adhesion(n=129)	0.687	0.625-0.748	<0.001	50.4	78.4
Severe adhesion(n=58)	0.786	0.727-0.846	<0.001	77.6	65.2

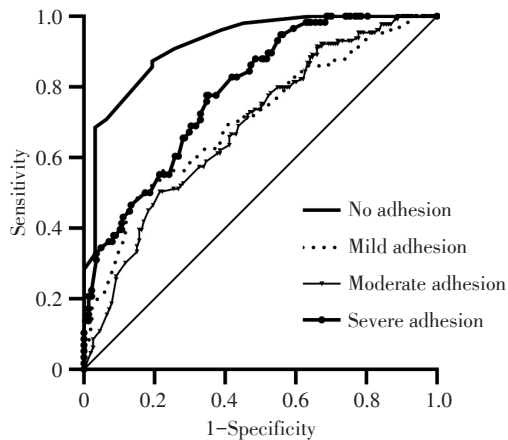


图2 HSG影像特征联合临床特征诊断IUA的ROC曲线

Figure 2 The ROC curve of HSG imaging features combined with clinical features in the diagnosis of IUA

2.4 HSG影像特征联合临床特征与三维超声诊断效能对比

以宫腔镜检查为金标准,对比分析HSG影像特征联合临床特征与三维超声(three-dimensional ultrasound, 3D ultrasound)诊断IUA的效能,共纳入164例患者。结果显示(表5、6),HSG影像特征联合临床数据在宫腔粘连患者中的诊断灵敏度为87.6%,准确度为86.6%,高于3D超声的灵敏度(81.4%)和准确度(79.9%)。但两种诊断方法的阴性预测值均相对较低,对排除IUA的可靠性有限。

3 讨论

研究报道,输卵管不通以及IUA是导致不孕症的重要原因^[13],合计占不孕症的比率为45%~

表5 HSG与三维超声诊断IUA的一致性比较

Table 5 Consistency comparison of IUA diagnosis between HSG and 3D ultrasound (n=164)

Gold standard	3D ultrasound		HSG combined with clinical features		Total
	Positive	Negative	Positive	Negative	
Hysteroscopy	IUA	118	27	127	145
	Non-IUA	6	13	4	19
	Total	124	40	131	33

表6 HSG联合临床特征与三维超声诊断IUA的效能比较

Table 6 Diagnostic performance of HSG combined with clinical features vs. 3D ultrasound for IUA (n=164)

Method	Sensitivity (%)	Specificity (%)	PPV (%)	NPV (%)	Accuracy (%)
HSG-CF	87.6	78.9	96.9	45.5	86.6
3D ultrasound	81.4	68.4	95.2	32.5	79.9

HSG-CF: HSG combined with clinical features; Sensitivity=true positive/(true positive+false negative); Specificity=true negative/(true negative+false positive); PPV=true positive/(true positive+false positive); NPV=true negative/(true negative+false negative); Accuracy=(true positive+true negative)/total cases.

50%^[14]。而目前能同时评估宫腔形态以及输卵管通畅性的无创且客观的操作检查仍然只有子宫输卵

管造影检查。目前HSG对输卵管通畅度检查效能高达94%^[15],而对IUA的讨论目前尚局限于单纯的影像形态学描述。因此,本研究旨在通过多因素有序Logistic回归分析和ROC曲线评估,系统探讨HSG影像学特征联合临床资料在评估IUA严重程度中的诊断价值,以期进一步提高HSG对IUA的检查效能。ROC结果表明其对IUA的灵敏度(87.3%)较高,适合作为存在多次宫腔操作并且需要同时评估输卵管状态的不孕患者的检查手段。本研究也证实了HSG影像学特征联合临床特征,能较为灵敏且准确地评估IUA的严重程度。

宫腔粘连综合征是指子宫腔内壁粘连,造成宫腔全部或部分闭塞,导致的一系列症状^[16]。IUA最常见的原因是宫腔操作后子宫内膜损伤,如人工流

产和反复刮宫术、子宫肌瘤剔除术、子宫纵隔切除术、剖宫产及上环取环等,使得子宫内膜与肌层过度创伤,特别是合并感染情况下,使子宫腔或宫颈管发生粘连。根据粘连程度与部位的不同,其临床表现各异,常见有月经量减少、痛经、闭经、反复流产及不孕等。本研究多因素分析结果显示,流产史、月经量减少及不孕为主要临床特征,与共识中的相关因素相吻合。另外本研究还发现,频繁的宫腔操作不仅导致IUA,还可能引起输卵管炎症性狭窄甚至闭塞不通。本研究显示,IUA患者输卵管异常发生率为39.8%,虽较文献报道的67.3%为低,但双侧输卵管阻塞则提示中重度IUA风险较高。IUA合并输卵管异常多由于IUA部位好发于两侧子宫角部,使得两侧输卵管开口被物理性堵塞,还可能与宫腔损伤引发炎症导致输卵管炎性闭塞而导致不孕^[17]。我国不孕患者中输卵管因素占比最高,而IUA也占子宫因素不孕的45.5%^[18],故本研究表明HSG检查能全面反映输卵管条件以及宫腔条件,为不孕症患者提供全面且客观的女性生殖系统检查。

子宫输卵管造影作为评估女性不孕症患者宫腔形态及输卵管通畅性的重要手段,其诊断效能受对比剂特性影响。既往研究证实,非离子型碘水对比剂可反映输卵管通畅性,但因流速快,对宫腔观察不佳^[19]。本研究采用罂粟乙碘油作为对比剂,由于碘油流速慢,且密度均匀,不仅能准确反映宫腔内密度差异,而且能显示宫腔及输卵管等诸多碘水难以观察到的微小细节,造影同时通过改变体位,可有效排除部分宫腔假阳性征象。但数据提示仍存在10.99%(31/282)的假阳性率,其原因可能与检查过程中子宫肌层痉挛导致宫腔局部狭窄或充盈不佳,造成粘连假象。HSG在联合临床特征后,显著提升对IUA的整体诊断效能。然而,其对宫颈管粘连的诊断存在局限性:宫颈钳夹牵拉及导管球囊置入可能扭曲宫颈的解剖形态,甚至改变原有粘连状态,导致假阴性率升高。尽管本研究证实HSG联合临床特征对IUA诊断表现出较高的灵敏度,且辐射剂量极低^[20],但其存在一定的辐射暴露,仍在一定程度上限制了临床应用。因此,在临床操作中,应严格评估,并在操作时采取合理防护措施,如非检查部位的辐射屏蔽遮挡以及缩小检查光栅等,将患者辐射剂量降至最低。本研究基于罂粟乙碘油对比剂在HSG检查中的应用,发现其影像特征包括充盈缺损的位置及数量、宫腔轮廓的不规则性以及双侧输卵管的梗阻情况。当HSG检查发现宫腔出

现以上影像学特征时,应警惕IUA的形成,同时结合临床特征,将能更为精准地诊断出IUA,减少患者重复检查以及指导后续治疗及生育计划。

超声检查因其无创且可重复成为女性IUA筛查的首选方法,其不仅能够评估子宫内膜厚度、宫腔形态而且还可以评估宫腔血流情况。然而,其诊断准确性受操作者经验、患者配合度及检查角度等多种因素限制。相比之下,HSG虽同样依赖操作者技术,但其影像图像结果更具客观可视性,且本中心每年有近3 000例HSG操作,诊断医生对HSG图像判读具有丰富的经验。研究发现三维超声对宫腔轻度粘连的敏感性较低,存在漏诊风险,影响患者后续的治疗^[21-22]。对比发现,HSG检查不仅能客观评估输卵管通畅性,还能对宫腔形态等进行检查,因此,本研究基于HSG影像特征联合临床特征对不孕症IUA患者具有较高的诊断价值。当然,三维超声联合彩色多普勒超声能为宫腔IUA检查提供一些补充诊断价值,其不仅能清晰显示宫腔形态异常,还能通过血流信号评估内膜活性,可用于比较治疗前后的差异和评估治疗效果^[7]。本研究中三维超声和HSG检查的阴性预测值相对较低(32.5%、45.5%),这表明可能由于样本量相对较少,或将一些宫腔内膜较厚的组织误诊为IUA,导致存在一定假阳性可能。但HSG检查在IUA的诊断中显示出更高的检出率和准确性,特别是在先天性子宫发育异常的诊断中,一定程度弥补了其阴性预测值相对低的问题。因此,HSG在低患病率人群中的表现仍需进一步验证。综上,HSG与三维超声的联合应用,既能发挥HSG在不孕症患者宫腔IUA的发现和分型中的优势,又能利用三维超声的无创特性实现长期随访,为IUA的诊疗策略提供可靠方案。

基于6项独立预测因子,对诊断及轻中度IUA分型展现出良好的鉴别能力(AUC>0.70),对中度粘连的预测能力一般,这可能与宫腔体积较小,影像学特征较难把握分类有关,后续应纳入更多的变量进行更为全面且充分的诊断。基于这些证据,HSG联合临床特征不仅可用于不孕症患者宫腔IUA的初步诊断,还可用于术前分层管理:对于预测为轻度的患者,应避免进行过度检查;而对于HSG显示存在中央型充盈缺损且合并双侧输卵管阻塞的患者,则应优先考虑转诊进行宫腔镜评估。此外,预测因子整合输卵管状态与宫腔形态参数,为不孕症提供一站式评估方案,弥补了传统方法仅关注单一器官的局限性。需注意的是,作为放射性检查,HSG应

用应严格遵循不孕症诊疗规范。

整合HSG影像特征与临床指标,可有效克服单一检查的局限性,进一步彰显HSG在IUA分型诊断中的独特优势。因此建议不孕症且怀疑存在IUA的患者建立阶梯式诊断流程:以HSG联合临床特征进行IUA诊断分型及输卵管通畅度评估,三维超声补充内膜血流分析,最终由宫腔镜确诊,从而平衡诊断效率与医疗成本。本研究存在的局限性:首先,回顾性研究设计可能存在选择偏倚;其次,未系统比较HSG与三维超声对不同分型IUA的鉴别能力。最后,本研究基于单中心数据,需多中心验证以提高外部适用性。后续将纳入更多预测因子(如炎症标志物等),提升对中度IUA的鉴别能力,并探索多模态诊断系统,结合HSG的形态特征与超声血流参数,以实现更为精确的无创评估,从而进一步丰富和完善IUA的个体化诊疗体系。

综上所述,本研究的HSG影像特征联合临床特征能很好地预测IUA的价值以及分型,有助于尽早识别IUA患者,并为其提供更为个性化的诊疗及助孕方案。

利益冲突声明:

所有作者声明无利益冲突。

Conflict of Interests:

The authors declared no competing interests.

作者贡献声明:

刘婷负责研究设计、数据收集整理与分析以及论文的撰写工作。杜子伟负责数据分析、论文修订。徐文健负责研究设计、论文审阅及修改、指导。鲁景元和李秀玲负责论文的审阅、指导。

Author's Contributions:

LIU Ting was responsible for research design, data processing and analysis, and manuscript drafting. DU Ziwei was responsible for data analysis and critical revision of the manuscript. XU Wenjian was responsible for study design, critical revision of the manuscript, and guidance on the research. LU Jingyuan and LI Xiuling were responsible for critical review of the manuscript and guidance.

[参考文献]

- [1] TAN J F, DENG M, XIA M, et al. Comparison of hysterosalpingography with laparoscopy in the diagnosis of tubal factor of female infertility [J]. *Front Med (Lausanne)*, 2021, 8: 720401
- [2] XIN L B, WEI C, TONG X M, et al. In situ delivery of apoptotic bodies derived from mesenchymal stem cells *via* a hyaluronic acid hydrogel: a therapy for intrauterine adhesions[J]. *Bioact Mater*, 2021, 12: 107-119
- [3] HOOKER A B, LEMMERS M, THURKOW A L, et al. Systematic review and meta-analysis of intrauterine adhesions after miscarriage: prevalence, risk factors and long-term reproductive outcome [J]. *Hum Reprod Update*, 2014, 20(2): 262-278
- [4] MORTIMER R M, LANES A, SROUJI S S, et al. Treatment of intrauterine adhesions and subsequent pregnancy outcomes in an *in vitro* fertilization population [J]. *Am J Obstet Gynecol*, 2024, 231(5): 536.e1-536.e10
- [5] TSAI N C, HSIAO Y Y, SU Y T, et al. The efficacy of early office hysteroscopy in preventing intrauterine adhesions after abortion: a randomized controlled trial [J]. *BMC Womens Health*, 2024, 24(1): 400
- [6] PENG E, ZENG Y Y, HE D, et al. Intrauterine infusion of autologous endometrial stem cells for the treatment of moderate and severe intrauterine adhesions: a before-and-after study [J]. *Stem Cell Res Ther*, 2025, 16(1): 219
- [7] ZHAO X P, GUAN X M, ZHANG B Y, et al. Three-dimensional transvaginal ultrasound offers superior live birth prediction after hysteroscopic adhesiolysis [J]. *Reprod Biomed Online*, 2025, 51(1): 104808
- [8] IGBODIKE E P, BADEJOKO O O, FASUBAA O B, et al. Correlation between hysterosalpingography diagnosis and final hysterolaparoscopy with dye-test diagnosis in women with utero-tubal infertility: a cross-sectional study of the implication for which test should be the first-line investigation [J]. *SAGE Open Med*, 2022, 10: 1-8
- [9] MATHEWS D M, PEART J M, SIM R G, et al. Iodine and other factors associated with fertility outcome following oil-soluble contrast medium hysterosalpingography: a prospective cohort study [J]. *Front Endocrinol (Lausanne)*, 2024, 15: 1257888
- [10] 王 银, 杜子伟, 徐文健, 等. 原发不孕症患者对不同碘油对比剂在子宫输卵管造影后结果的比较分析 [J]. *实用放射学杂志*, 2024, 40(9): 1514-1517
WANG Y, DU Z W, XU W J, et al. Comparison analysis of the results of hysterosalpingography with different iodized oil-based contrast medium in primary infertility patients [J]. *Journal of Practical Radiology*, 2024, 40(9): 1514-1517
- [11] TOMA L M, SOCOLOV D, MATEI D, et al. Intrauterine adhesions and asherman syndrome: a retrospective dive into predictive risk factors, diagnosis, and surgical perspectives [J]. *Diagnostics (Basel)*, 2025, 15(8): 955
- [12] The American Fertility Society classifications of adnexal adhesions, distal tubal occlusion, tubal occlusion secondary to tubal ligation, tubal pregnancies, müllerian anomalies and intrauterine adhesions [J]. *Fertil Steril*, 1988, 49(6): 944-955

- [13] 王 峥,张琪琪,张 桐,等. 不孕症患者慢性子宫内膜炎与输卵管性疾病的相关性分析[J]. 生殖医学杂志, 2024, 33(1): 23-28
WANG Z, ZHANG Q Q, ZHANG T, et al. Analysis of correlation between chronic endometritis and tubal disease in infertile patients [J]. Journal of Reproductive Medicine, 2024, 33(1): 23-28
- [14] TOUFIG H, BENAMEUR T, TWFIG M E, et al. Evaluation of hysterosalpingographic findings among patients presenting with infertility [J]. Saudi J Biol Sci, 2020, 27(11): 2876-2882
- [15] KAMPHUIS D, VAN EEKELLEN R, VAN WELIE N, et al. Hysterosalpingo - foam sonography versus hysterosalpingography during fertility work-up: an economic evaluation alongside a randomized controlled trial[J]. Hum Reprod, 2024, 39(6): 1222-1230
- [16] QIAO X Y, LIU D, LIU C, et al. Reproductive outcomes after hysteroscopic adhesiolysis in patients experiencing recurrent pregnancy loss and intrauterine adhesions[J]. J Minim Invasive Gynecol, 2025, 32(1): 57-63
- [17] MAYRHOFER D, HOLZER I, ASCHAUER J, et al. Incidence and causes of tubal occlusion in infertility: a retrospective cohort study[J]. J Clin Med, 2024, 13(13): 3961
- [18] 李博涵,段 华. 子宫内膜损伤子宫腔结构异常的诊治与生育功能评估[J]. 中国实用妇科与产科杂志, 2025, 41(3): 284-289
LI B H, DUAN H. Diagnosis and treatment of structural abnormalities of uterine cavity with endometrial injury and evaluation of reproductive function [J]. Chinese Journal of Practical Gynecology and Obstetrics, 2025, 41(3): 284-289
- [19] 中国妇幼保健协会放射介入专业委员会. 输卵管造影技术规范中国专家共识(2022年版)[J]. 中国实用妇科与产科杂志, 2022, 38(2): 165-169
Radiological Intervention Committee of China Maternal and Child Health Association. Chinese expert consensus on technological standards for salpingography (2022) [J]. Chinese Journal of Practical Gynecology and Obstetrics, 2022, 38(2): 165-169
- [20] KLANGSIN S, MATEMANOSAK P, PEEYANANJARASSRI K, et al. Effect of radiation on serum anti-Müllerian hormone during hysterosalpingography in female infertility [J]. Reprod Biomed Online, 2024, 48(6): 103843
- [21] MAHUTTE N, HARTMAN M, MENG L, et al. Optimal endometrial thickness in fresh and frozen-thaw *in vitro* fertilization cycles: an analysis of live birth rates from 96 000 autologous embryo transfers [J]. Fertil Steril, 2022, 117(4): 792-800
- [22] ATA B, LIÑÁN A, KALAFAT E, et al. Effect of the endometrial thickness on the live birth rate: insights from 959 single euploid frozen embryo transfers without a cutoff for thickness[J]. Fertil Steril, 2023, 120(1): 91-98
(收稿: 2025-07-04; 修回: 2025-10-24; 录用: 2025-10-28)
(本文编辑: 戴王娟)